BJD
British Journal of Dermatology

Surface air plasma-induced cell death and cytokine release of human keratinocytes in the context of psoriasis*

S.Y. Zhong,[1,2] Y.Y. Dong,[1,2] D.X. Liu,[2,3] D.H. Xu,[2] S.X. Xiao,[1] H.L. Chen[4] and M.G. Kong[2,3,4]

[1]Department of Dermatology; [2]Center of Plasma Biomedicine, State Key Laboratory of Electrical Insulation and Power Equipment and [3]School of Electrical Engineering; Xi'an Jiaotong University, Xi'an 710049, China
[4]Center for Bioelectrics, Old Dominion University, Norfolk, VA 23508, U.S.A.

Linked Comment: Lunov. *Br J Dermatol* 2016; **174**:486–487

Correspondence
Yingying Dong and Michael G. Kong.
E-mails: dyingying97@163.com; mglin5g@gmail.com

Accepted for publication
14 October 2015

Funding sources
This work was supported by the National Natural Science Foundation of China (grant no. 51221005) and Fundamental Research Funds for the Central Universities and State Key Laboratory of Electrical Insulation and Power Equipment (grant no. EIPE14129).

Conflicts of interest
None declared.

*Plain language summary available online

DOI 10.1111/bjd.14236

Summary

Background Cold atmospheric plasma (CAP) has shown promise for wound healing, although little is understood of the underpinning mechanisms. Little has been reported so far of its potential use in the treatment of immune-mediated diseases such as psoriasis.
Objectives To study CAP-induced cell death and cytokine release in human keratinocytes as a first assessment of possible CAP use for psoriasis.
Methods Using a CAP generator free of energetic ions, we observed its effects on keratinocytes in terms of morphology, cell viability and apoptosis, intracellular and mitochondrial reactive oxygen species (ROS), lysosomal integrity and mitochondrial membrane potential; and on secretion and expression of eight cytokines at protein and gene levels.
Results CAP-induced reduced cell viability, apoptotic death and production of intracellular and mitochondrial ROS in dose-dependent manner. Mitochondrial dysfunction and lysosomal leakage were found in CAP-treated cells. It also induced release of interleukin (IL)-6, IL-8, tumour necrosis factor (TNF)-α and vascular endothelial growth factor (VEGF), and enhanced the mRNA expression of IL-1β, IL-6, IL-8, IL-10, TNF-α, interferon-γ and VEGF. By contrast, IL-12 declined monotonically.
Conclusions The results suggest that with appropriate control of its dose, physical plasma could induce cell death via apoptotic pathways and enable simultaneous reduction in IL-12. These effects may be used to suppress keratinocyte hyperproliferation and to target T-cell activation to control amplification of inflammation. This provides an initial basis for further studies of CAP as a potential therapeutic option for inflammatory and immune-related diseases in dermatology, including psoriasis.

What's already known about this topic?

- Cold atmospheric plasma (CAP) is effective for wound healing.
- CAP can induce apoptotic death in some skin cells.

What does this study add?

- CAP induced apoptosis, mitochondrial dysfunction and lysosomal leakage in HaCaT cells.
- CAP-induced release of cytokines is dose dependent and cytokine specific, thus enabling preferential targeting. Its reduction of interleukin-12 may be used to target suppression of T cells.
- Our study provides an *in vitro* basis for CAP as a possible therapeutic option for psoriasis.

Nonthermal atmospheric-pressure plasma, also known as cold atmospheric plasma (CAP), has recently found successful applications in medicine.[1] Examples include instrument sterilization,[2] tissue disinfection,[3] treatment of pruritus,[4] wound healing[5] and cancer therapy.[6] With some applications having already completed or undergoing clinical trials,[3–5] CAP devices appear to be well suited for dermatology.[7] It is known that CAP delivers a cocktail of reactive oxygen species (ROS), reactive nitrogen species (RNS) and low fluxes of photons, which are known to be effective for treating skin diseases.[8,9] However, little is currently understood of the cellular components and functions affected by CAP, and this is impeding the realization of its potential for dermatology.

Probably the most prevalent immune-mediated skin disease in adults, psoriasis, is caused by the activation of T cells and/or B cells without ongoing infection.[10] It is associated with keratinocyte hyperproliferation and inflammatory infiltration. Despite considerable advances in the understanding of psoriasis pathogenesis, much needs to be learned in terms of its key cellular interactions and molecular pathways of inflammation. Detailed *in vivo* studies are impeded by a lack of animal models that faithfully reproduce human psoriasis.[10]

Our motivation for using physical plasmas as a possible therapy for psoriasis is based on two considerations. Firstly, CAP can be applied locally to psoriatic areas similarly to ultraviolet (UV)B phototherapy,[9–11] and secondly, ROS are an effective way of inhibiting T cells.[12] Detailed evaluation of this possibility has not been reported previously, and so it seems appropriate to start with an *in vitro* evidence-gathering study with which to inform more focused studies in the future. To this end, our objectives were to investigate (i) cell death, to assess CAP suppression of keratinocyte hyperproliferation and release of cytokines involved in inflammation development, and (ii) the effects of physical plasmas on inflammatory and immunological functions. This study uses the immortalized human keratinocyte (HaCaT) cell line, as it shares similar characteristics of differentiation and proliferation to normal human keratinocytes and is the most commonly used cell model for psoriasis studies.[13]

As a reference, physical plasmas have been studied for treatment of skin diseases, mostly melanoma[14–16] and chronic wounds,[17–23] with a focus on apoptosis, adhesion molecules, cell cycles, the transcriptome and roles of ROS. There are very few studies on immunological responses, with evidence for leakage of nucleic acids and potassium,[24] denaturation of adhesion molecules[25] for lymphocytes, and expression of genes relevant to wound healing for dermal fibroblasts.[16] These are too few to support a coherent picture of CAP-induced immunological responses.

Materials and methods

Cells and cell culture

HaCaT cells were purchased (Cell Resource Center, Peking Union Medical College, Beijing, China) and grown in MEM-EBSS medium (minimum essential medium/Earle's balanced salt solution; GE Healthcare, Little Chalfont, U.K.) supplemented with 10% fetal bovine serum (Life Technologies, Grand Island, NY, U.S.A.) and 1% penicillin–streptomycin solution (PAA, Linz, Austria). They were then subcultured routinely using 0·25% trypsin/ethylenediaminetetraacetic acid solution (GE Healthcare). The cells were confirmed as being mycoplasma free with real-time polymerase chain reaction (PCR). HaCaT cells from 10–30 passages in the log growth phase were used in our study. Keratinocytes from patients with psoriasis were found to become normal keratinocytes easily *in vitro* after several passages, thus offering little support for their use in this study.

Plasma device and treatment of cells

With details reported elsewhere,[26] a dielectric-barrier discharge (DBD) generator was used to produce a room-temperature and stable surface air plasma sustained with an electrical power of 0·06 W cm^{-2}. At the sample point, it had a photon flux density (3·2 μW cm^{-2}) mostly in the UVB band, four to five orders of magnitude less than those used in UVB phototherapy. The surface air plasma imposed negligible thermal burden on and no flux of ions and electrons to the downstream sample. The surface DBD generator is integrated into a closed treatment cavity with a Petri dish placed 10 mm away (Fig. 1). In order to protect cells from dehydration during treatment, HaCaT cells adhered with phosphate-buffered saline (PBS; Corning Inc., Corning, NY, U.S.A.) were exposed to the plasma. Immediately after plasma treatment, PBS was replaced by fresh culture medium. Plasma treatment experiments were repeated independently at least three times.

Morphological observations

The general and ultrastructural changes on cell morphology were imaged 24 h after plasma treatment. The cells in the

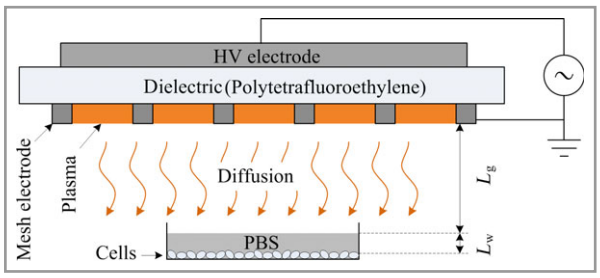

Fig 1. Schematic set-up of the surface dielectric-barrier discharge source and the cell sample under treatment. The electrical power density is 0·06 W cm^{-2}. The ultraviolet (UV) power density is 3·2 μW cm^{-2}, mostly in the UVB band. The air gap between the electrode and the sample is adjusted to $L_g \approx 10$ mm and the depth of phosphate-buffered saline (PBS) above the cells is $L_w \approx 1$ mm. In the experiments, the air plasma generates active species including reactive oxygen and nitrogen species, some of which transport across the air gap and then penetrate into the PBS.

Petri dish were used directly for light microscopic observation (IX51; Olympus, Center Valley, PA, U.S.A.). The protocol of the transmission electron microscope (TEM) was as follows. Trypsinized HaCaT cells were collected and centrifuged at 3000 **g** for 10 min after washing three times with cold PBS. Pellets were fixed by immersion in 2·5% glutaraldehyde for 24 h at 4 °C. The samples were then fixed with osmium tetroxide and dehydrated through an increasing graded ethanol series, before being embedded with epoxy resin Epon 812. Ultrathin sections were cut and then stained with uranyl acetate and lead citrate. TEM (H7650; Hitachi, Tokyo, Japan) was used to explore the ultrastructural changes.

Cell viability measurement

To measure cell viability, 6000 cells per well were seeded in 96-well plates with five replicates the day before CAP treatment. To clarify the role of UV generated from the plasma, a quartz plate was placed above the 96-well plate to let the UV emission through but not gaseous plasma species. The antioxidant N-acetyl-L-cysteine (NAC; Sigma-Aldrich Co., St Louis, MO, U.S.A.) at 10 mmol L^{-1} concentration was added to the culture medium 0·5 h before the plasma treatment in order to establish the effect of ROS. Cell viability was assessed using the Cell Counting Kit-8 (CCK-8; 7sea Biotech, Shanghai, China). A 10-μL aliquot of CCK-8 solution per 100 μL culture medium was added to each well at 4, 24, 48 and 72 h after treatment. After incubation for 2 h, the light absorbance at 450 nm was recorded by a microplate reader (3001; Thermo Scientific, Waltham, MA, U.S.A.).

Apoptosis assay

Cells were collected 16 h after CAP treatment for the apoptosis assay using the Annexin V-FITC Apoptosis Detection Kit I (BD Biosciences, San Jose, CA, U.S.A.). Cells that stained negative for both annexin V–fluorescein isocyanate (FITC) and propidium iodide (PI) were alive without measurable apoptosis; early apoptosis cells stained annexin V–FITC positive and PI negative; and late apoptosis and dead cells stained both annexin V–FITC and PI positive. The arrays were conducted according to the manufacturer's instruction within 1 h after staining. Apoptotic cells were detected by flow cytometer (Accuri C6; BD Biosciences).

Hydrogen peroxide and total nitrate/nitrite detection in plasma-treated phosphate-buffered saline

The concentration of H_2O_2 in plasma-treated PBS was measured using a colorimetric assay (Amplex® Red Hydrogen Peroxide/Peroxidase Assay Kit; Invitrogen, Carlsbad, CA, U.S.A.). H_2O_2 molecules in the sample react with the Amplex Red reagent and horseradish peroxidase, and the resulting fluorescence is measured by a microplate reader equipped for excitation at a wavelength of 540 nm and emission at 590 nm. Detection of the total nitrate and nitrite concentration was carried out using a nitrate/nitrite colorimetric assay kit (Cayman, Ann Arbor, MI, U.S.A.). Using nitrate reductase to convert nitrate to nitrite, the total concentration of nitrate and nitrite was determined using the NO_2^- concentration. The absorbance at 540 nm was measured and calculated in comparison with the standard curve from the manufacturer.

Intracellular and mitochondrial reactive oxygen species

The fluorescent probe 2′,7′-dichlorofluorescin diacetate (DCFH-DA; Sigma-Aldrich) was used to detect intracellular ROS levels. Briefly, 2 h after the plasma treatment, HaCaT cells were incubated with 1 mL PBS containing 10 μmol L^{-1} DCFH-DA for 30 min. After washing with PBS three times, cells were collected for flow cytometry within 1 h. For mitochondrial ROS detection, mitochondria were extracted from cells with 3-min plasma treatment using a high-purity mitochondria isolation kit (GenMed Scientifics Inc., Wilmington, DE, U.S.A.). The staining process was the same as mentioned above.

Lysosomal leakage

Cells in the 35-mm dish were cultured overnight with 100 μg mL^{-1} Lucifer yellow (Sigma-Aldrich) mixed in the medium. Next, 24 h after plasma treatment, cells were washed with PBS three times and observed by fluorescence microscope (Olympus).

Mitochondrial membrane potential

The mitochondrial membrane potential (MMP) of HaCaT cells was detected by JC-1 (5,5′,6,6′-tetrachloro-1,1′,3,3′-tetraethylbenzimidazolocarbocyanine iodide) probe of a mitochondria staining kit (Sigma-Aldrich). Cells cultured in 35-mm dishes after plasma treatment were incubated with medium containing 2·5 μg mL^{-1} JC-1 staining solution at 37 °C for 20 min. After washing with medium twice, cells in the culture dishes were used directly for fluorescence microscopy. Collected cells suspended in ice-cold staining buffer were measured by flow cytometric assays. Cells pretreated with valinomycin acted as the positive control.

Activity of caspase-3 and caspase-9

The cellular activities of caspase-3 and caspase-9 with 3-min plasma treatment were determined by colorimetric assay kit (Biovision, Milpitas, CA, U.S.A.). Cell lysates were prepared from the cell lysis buffer at 3, 6, 9 and 12 h after plasma treatment. Assays were performed in 96-well plates with 150 μg protein and 50 μL reaction buffer containing 10 mmol L^{-1} dithiothreitol. A 5-μL aliquot of 4 mmol L^{-1} DEVD-*p*NA (for caspase-3) or LEHD-*p*NA (for caspase-9) was added to the wells. After incubating at 37 °C for 2 h, the absorbance was measured at 405 nm. The result was calculated by the ratio of treated cells to untreated cells (i.e. vs. the control).

Cytokine release and mRNA expression

Culture supernatants were collected for cytokine assay, 24 h after CAP treatment, by quantitative sandwich enzyme-linked immunosorbent assay (ELISA). The kits for interleukin (IL)-1β, IL-6, IL-8, IL-10, IL-12, tumour necrosis factor (TNF)-α, interferon (IFN)-γ and vascular endothelial growth factor (VEGF) were purchased from R&D Systems Inc. (Minneapolis, MN, U.S.A.). A microplate reader set to 450 and 540 nm was used for the absorbance observation. The concentration of the sample was obtained through the establishment of standard curves.

Real-time quantitative PCR was used for detection of mRNA expression of cytokines. Briefly, cells were collected for total RNA extraction by Trizol reagent (Invitrogen). RNA (1 μg) in 20 μL reaction system was used for reverse-transcriptase cDNA synthesis (Revert Aid First Strand cDNA Synthesis Kit; Thermo Scientific). The products were amplified with suitable primers (Sangon Biotech, Shanghai, China) and SYBR Green I fluorescent dye (Applied Biosystems, Foster City, CA, U.S.A.). The primer sequences are listed in Table S1 (see Supporting Information). The results were normalized to β-actin using the $2^{-\Delta\Delta C_t}$ method. Experiments under each condition were conducted in triplicate independently.

Statistical analysis

All experiments were performed independently at least three times. Descriptive data are expressed as mean ± SD. Statistical analyses were performed in SPSS 13.0 (IBM, Armonk, NY, U.S.A.) using the t-test and Kruskall–Wallis test, followed by the Mann–Whitney U-test. Statistical significance of data was established at $P < 0{\cdot}05$.

Results

Morphological observations

Within 2 min of plasma treatment, cells showed mild changes of morphological characteristics, as shown in Figure 2. With plasma treatment extended to 3 min, the appearance of cell shrinkage and membrane bleb formation was observed, with some cells detached from the plate walls. At 4 min, cellular structures were clearly destroyed and appeared to be frozen on the surface of the dish.

The ultrastructure of untreated HaCaT cells under the TEM is shown in Figure 2(f), with a large shape, more microvilli on the surface, uniform distribution of chromatin in the nucleus and clear mitochondrial crest structure. Plasma-treated cells showed clear morphological changes including short and less microvilli, swelling mitochondria and vacuolated mitochondrial crest. There were far more cells with cytoplasmic vacuolization and chromatin condensation with 3-min treatment than after 2 min, showing a typical apoptotic change. However, 4-min exposure led to swelling of cells with fragmented membrane and naked nucleus.

Cell viability

When observed at 4 h after the treatment, plasma treatment of no more than 2 min showed no obvious change in cell viability (Fig. 3). With the treatment time extended to 3 min, cell viability underwent a statistically significant decrease compared with the control ($P < 0{\cdot}001$), and there was a further reduction after 4 min ($P < 0{\cdot}001$). Data for 24 h post-treatment suggest that 1-min exposure led to minor reduction of cell viability, and longer treatment time resulted in a statistically significant

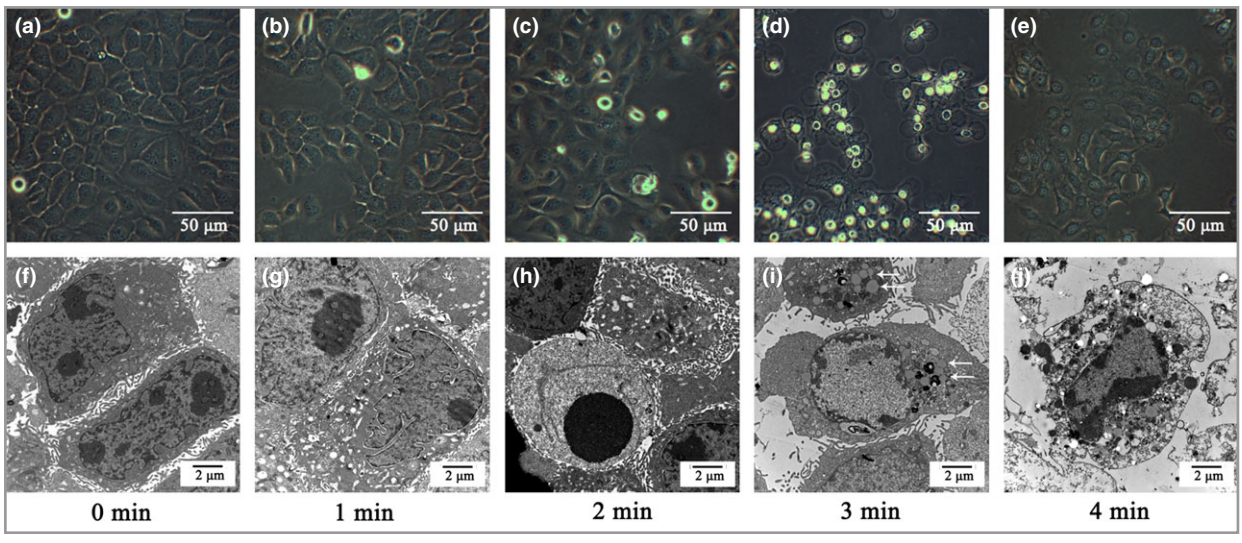

Fig 2. Morphological change of HaCaT cells without and with plasma treatment after 24-h cultivation under inverted optical microscopy (a–e) and electron microscopy (f–j). Cytoplasmic vacuolization (arrows) was more common in the 3-min treated cells, whereas a fragmented membrane and naked nucleus were found in cells with 4-min plasma treatment.

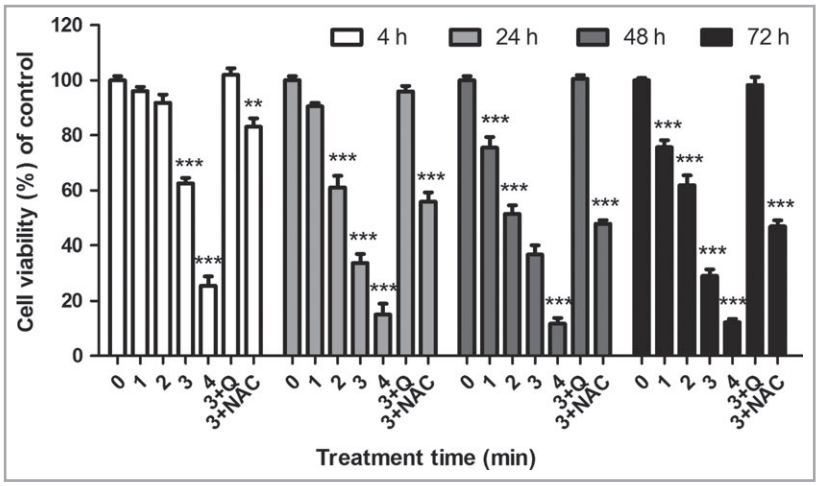

Fig 3. Cell viability of HaCaT cells 4, 24, 48 and 72 h after plasma treatment with surface air plasma. The antioxidant N-acetyl-L-cysteine (NAC), 10 mmol L^{-1}, is added in order to observe the effect of reactive oxygen species. 3+Q denotes 3−min plasma treatment with a covered quartz plate. 3 + NAC denotes 3-min plasma treatment with NAC added to the medium. The percentage cell viability is determined by normalization of the absorbance intensity to the untreated cells in each group. **P < 0·01, ***P < 0·001.

and progressively larger reduction. In general, these reductions became greater at 48 and 72 h after plasma treatment. No significant difference was observed with cells covered with a quartz plate as compared with the control. The addition of the antioxidant NAC was found to arrest the decrease in viable cells.

Apoptosis

As shown in Figure 4, the increasing percentage of apoptotic cells was significant in the 2-min treated group ($P < 0{\cdot}01$), and more notable in the 3-min group ($P < 0{\cdot}001$), while a minor change was seen in the 1-min group 16 h after the treatment. For the 4-min treatment, trypan blue staining showed all dead cells (Fig. S1; see Supporting Information), and flow cytometry showed that > 90% of the cells were both annexin V–FITC and PI positive. We suspected that cell death by 4-min plasma treatment was through necrotic rather than apoptotic pathways. The group with the antioxidant NAC added showed a lower percentage of apoptotic cells. Plasma treatment at a certain dose could induce apoptosis of HaCaT cells, and excessive treatment could lead directly to necrocytosis. The addition of NAC could mitigate or even inhibit the occurrence of apoptosis.

Hydrogen peroxide and total nitrate/nitrite detection in plasma-treated phosphate-buffered saline

As the biological effects of near room-temperature plasmas occur mainly through ROS and RNS, we measured concentrations of H_2O_2 and total nitrate/nitrite in plasma-treated PBS as being representative of plasma ROS and RNS experienced by cells in PBS. As shown in Figure 5, no H_2O_2 or nitrite was detected in untreated PBS, but their concentrations increased persistently with increasing plasma treatment time.

Intracellular and mitochondrial reactive oxygen species levels

Intracellular ROS levels in HaCaT cells were measured by DCFH-DA, a dye that shows cellular fluorescence intensity with intracellular ROS. As shown in Figure 6(a), plasma treatment significantly increased the intracellular ROS level, and the rising trend was obvious with increasing plasma treatment time. Addition of the ROS scavenger NAC was found to reduce significantly the level of intracellular ROS induced by the air plasma. To determine the mitochondrial ROS level, mitochondria from cells with 3-min plasma treatment were extracted for detection. Consistently with the intracellular ROS result above, plasma treatment led to an increase of mitochondrial ROS level compared with the control (Fig. 6b).

Lysosomal leakage

The pinocytic tracer Lucifer yellow was used to examine whether lysosomal leakage was induced by plasma treatment. As shown in Figure 7, untreated HaCaT cells displayed a discrete punctuate localization of fluorescence confirming that Lucifer yellow was circumscribed in intact lysosomes. For cells with 3-min plasma treatment, a diffuse distribution of fluorescence throughout the cell body was exhibited, which indicated lysosomal leakage into the cytosol owing to disruption of the permeability of the lysosomal membrane.

Mitochondrial membrane potential

The dissipation of the mitochondrial electrochemical potential gradient ($\Delta\psi_m$) is known as an early event in apoptosis. In untreated HaCaT cells, the dye JC-1 concentrated in the mitochondrial matrix to form red fluorescent aggregates due to the mitochondrial potential gradient. The shift from red aggregates to green monomers indicated the dissipation of the MMP that prevented the accumulation of JC-1 in the mitochondria. For cells with 3-min plasma treatment, Figure 8 displays the process from red aggregates to green monomers, demonstrating the impairment of the MMP.

Activity assay for caspase-3 and caspase-9

As an initiator and executor of cell death, the activation of cysteine proteases is involved in the process of apoptosis. As

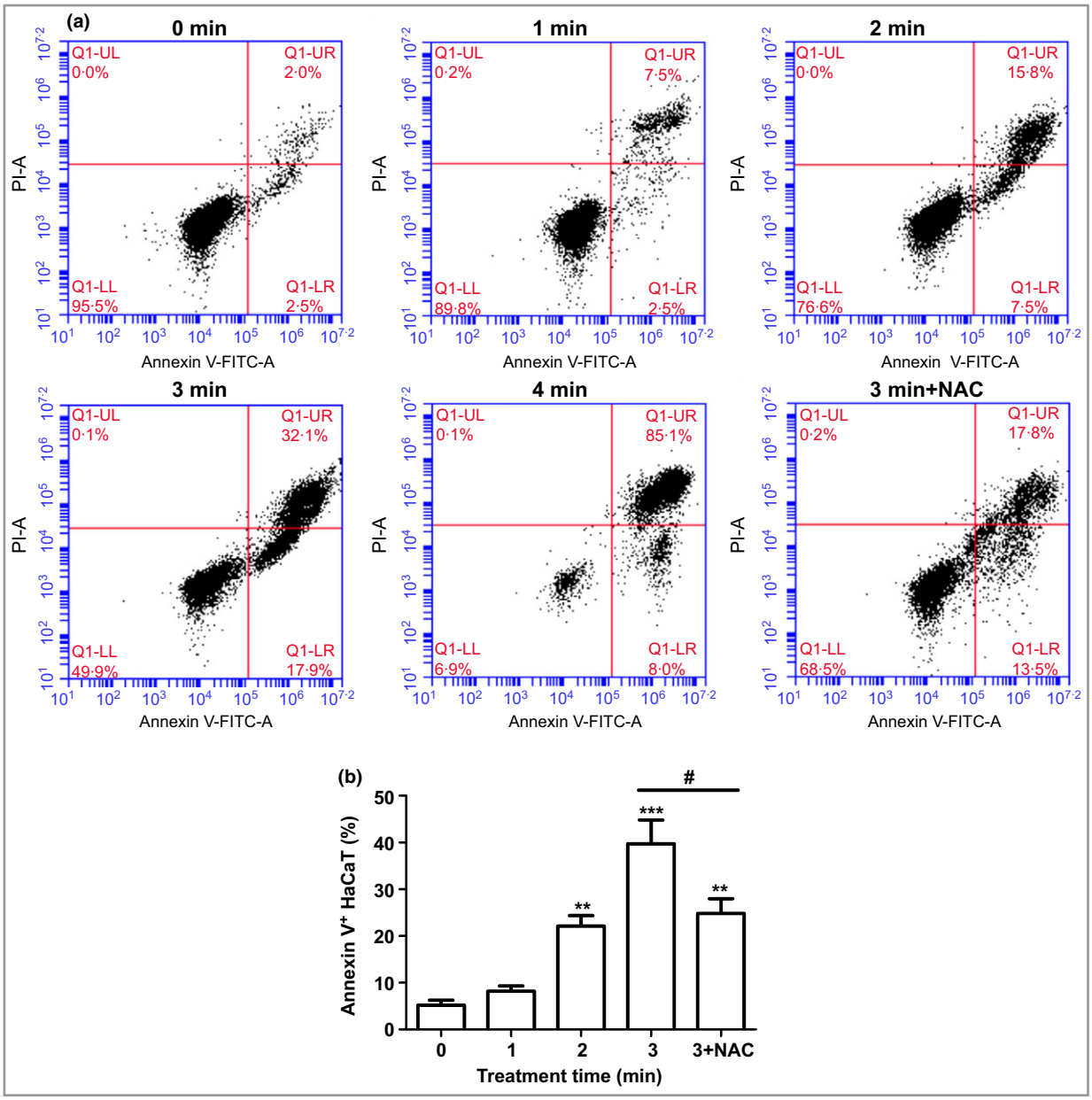

Fig 4. (a) Fluorescence-activated cell sorting analysis using Annexin V-FITC Apoptosis Detection Kit at 16 h after the plasma treatment, showing a progressive evolution of cells from early to late apoptosis at 16 h after plasma treatment. (b) The apoptotic cell population as a function of the plasma treatment time. NAC, antioxidant N-acetyl-L-cysteine. #$P < 0{\cdot}05$, **$P < 0{\cdot}01$, ***$P < 0{\cdot}001$.

shown in Figure 9, 3-min plasma treatment caused a time-dependent increase in caspase-3 and caspase-9 activities. Caspase-3 activity increased at 3 h after treatment and was maintained at a relatively high level until 9 h, after which a small decrease occurred until 12 h post-treatment. For caspase-9, a significant increase was found 3 h after plasma treatment and a gradual decay followed.

Cytokine release and mRNA expression

The concentrations of cytokines in the culture supernatants from plasma-treated and control cells were determined 24 h after treatment (Table 1). Unstimulated HaCaT cells secreted a certain amount of IL-6, IL-8 and VEGF, but only low levels of IL-12 and TNF-α. Plasma treatment induced a significant increase in the levels of IL-6, IL-8 and VEGF. Different cytokines appeared to increase after slightly different treatment times, for example 3 min for IL-6, 2 min for IL-8 and 1 min for VEGF. For IL-12, all of the treated groups showed a statistically significant decline. Although seen in all groups at low levels, the release of TNF-α in the 3-min treated group was significantly increased versus control. The secretions of IL-1β, IL-10 and IFN-γ were too low to be determined in either the control or plasma-treated groups.

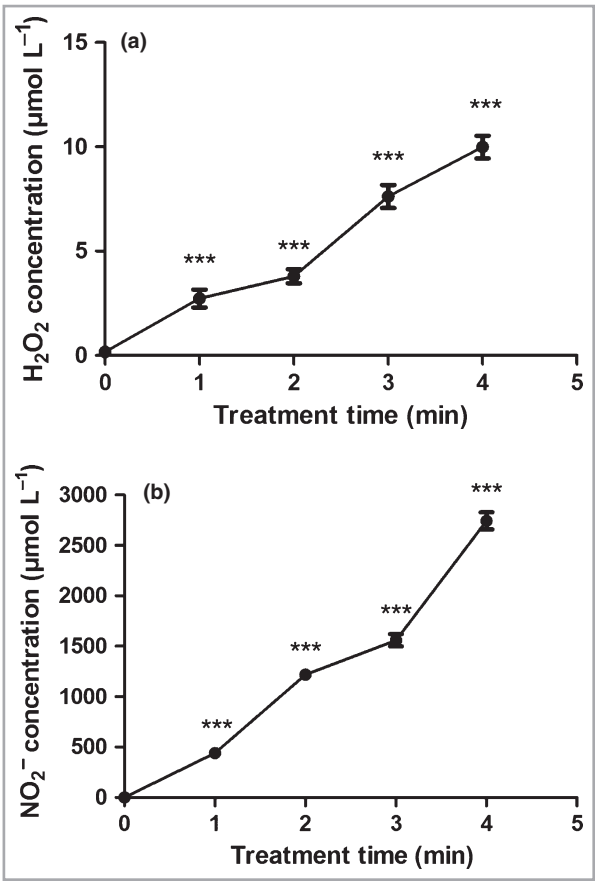

Fig 5. The concentration of (a) H_2O_2 and (b) total nitrate/nitrite in the plasma-treated phosphate-buffered saline. ***P < 0·001.

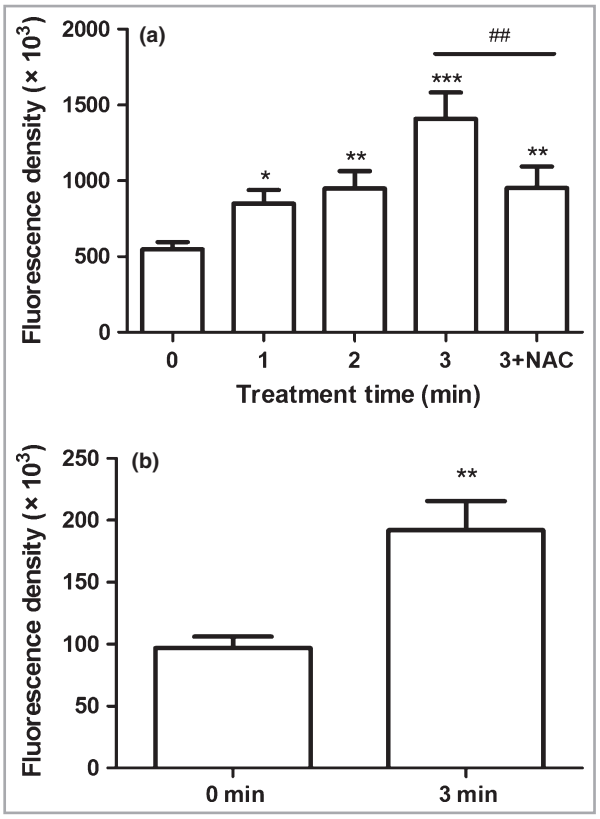

Fig 6. DCFH-DA (2′,7′-dichlorofluorescin diacetate) fluorescent assay. (a) Determination of intracellular reactive oxygen species (ROS) level, for which 3+NAC represents the case of 3-min plasma treatment with N-acetyl-L-cysteine added to the medium. (b) Determination of mitochondrial ROS level. *P < 0·05, **P < 0·01, ***P < 0·001, ##P < 0·01.

For mRNA expression of cytokines, the data in Figure 10 show a very similar trend consistent with the results of ELISA. Besides a reduced expression for IL-12 mRNA, the other cytokines from plasma-treated cells all appeared to follow a trend for increased mRNA expression of varying degrees.

Discussion

Of many variants of CAP used for treatment of cells and living tissues, a distinction may be made in terms of whether part of the electrical current flows through the sample. When a sample is in the current path, it is mostly exposed to high fluxes of energetic ions and UV photons. For psoriasis, our considerations are to minimize the possibly damaging effects of the energetic ions and UV photons of CAP, and to use ROS and RNS as the main plasma agents to achieve and optimize deactivation of keratinocyte hyperproliferation and suppression of inflammation amplification. The design of the surface air DBD shown in Figure 1 minimizes the contribution of ions and electrons, with the optical intensity of UV photons kept below 3·2 μW cm^{-2}. This is a very low-energy device, with its biological effects occurring mostly through ROS/RNS as confirmed by the detection of H_2O_2 and total nitrate and nitrite in the plasma-treated PBS. This surface air plasma device is physically scalable to treat large skin areas.[26]

Similar to other studies of plasma treatment of HaCaT cells,[17–20,23] our results show that physical plasma has an inhibitory effect on HaCaT cell viability in a dose-dependent fashion. This is supported by ultrastructural changes including cell-membrane shrinkage, microvilli shortening, mitochondria swelling, cytoplasmic vacuolization and chromatin condensation. Reduction of cell viability was accompanied by evolution of cells from a stage of annexin V–FITC and PI negativity at 4 h to annexin V–FITC positivity at 16 h. Excessive exposure led to necrocytosis directly. Notwithstanding the difference between HaCaT cells and psoriatic keratinocytes, and the need for *in vivo* studies, the above data appear to support the use of CAP to suppress and control keratinocyte hyperproliferation.

Apart from electrons and energetic ions, UV emission from the surface air plasma under experimental conditions reported here has a negligible effect on cell viability. By contrast, plasma treatment induces an increase of both intracellular and mitochondrial ROS levels. Introduction of the antioxidant NAC to the cell-containing media leads to a reduction in intracellular ROS levels and apoptotic cells, as well as an increase in cell viability. These findings are consistent in establishing that plasma ROS/RNS play the dominant role in plasma-mediated

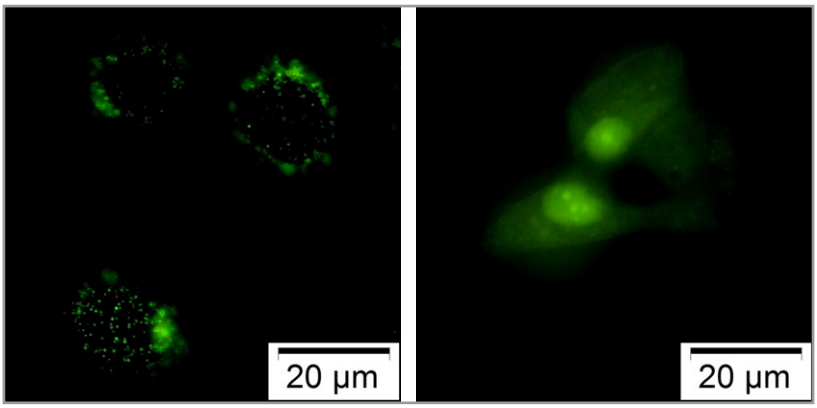

Fig 7. Plasma treatment induced the release of Lucifer yellow from lysosomes of HaCaT cells. Left: untreated HaCaT cells as the control, showing a discrete punctate localization of fluorescence. Right: HaCaT cells with 3-min plasma treatment display a diffuse distribution into the cytoplasm. The diffuse fluorescence staining of the pinocytic tracer Lucifer yellow indicates lysosomal leakage.

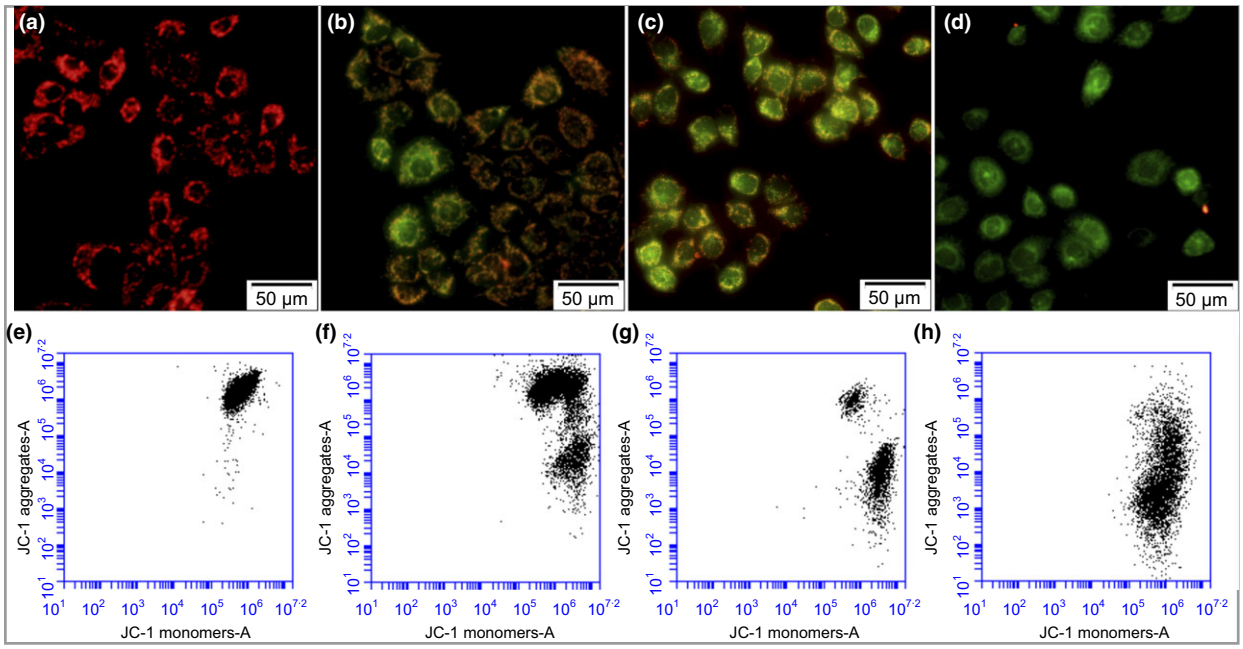

Fig 8. Mitochondrial membrane potential affected by plasma treatment. HaCaT cells stained with the reporter dye JC-1 for mitochondrial condition are determined by fluorescence microscopy (a–d) and flow cytometry (e–h). In untreated HaCaT cells (a, e) the dye forms red fluorescent aggregates. Valinomycin-treated cells (d, h), as the positive control, show cytoplasmic diffusion of green fluorescent monomers. Cells with 3-min plasma treatment (b, f, 6h after the treatment and c, g, 16h after the treatment) show a shift from red (JC-1 aggregates) to green fluorescence (JC-1 monomers), suggesting dissipation of mitochondrial membrane potential.

cellular effects. At a molecular level, our results show that plasma treatment can evoke the dissipation of the MMP, leading to mitochondrial dysfunction.[27] Lysosomal leakage in the form of rupture of lysosomal integrity is evident also, and could promote ROS production in mitochondria.[28] Furthermore, accumulation of superoxide could further result in dysfunction of mitochondria and lysosomes.[29] The observation of plasma-mediated increase in mitochondrial ROS supports the lysosomal leakage and MMP data. Given that mitochondria are the main site for apoptosis induction and are also a major source of cellular ROS, the plasma-induced increase of mitochondrial ROS production may have activated signalling pathways for mitochondria-localized apoptosis, consequently leading to the occurrence of apoptosis.[30]

In response to a variety of stimuli, the complex mechanism of intracellular inflammatory signal transmission of keratinocytes is activated with expression and secretion of inflammatory cytokines,[31,32] including IL-1, IL-6, IL-8, IL-10, TNF-α and granulocyte–macrophage colony-stimulating factor. These cytokines can affect the proliferation, differentiation and cell death of keratinocytes, and can increase or decrease the secretion of the cytokines.[33] Changes in cytokine secretion are involved in the occurrence, development and healing process of diseases such as lichen planus and psoriasis and in wound healing.

It is reported that inflammatory cytokines are linked to mitochondrial ROS production.[34] The present work employed a group of cytokines to gain a first understanding of their possible release by CAP, and the dependence of released

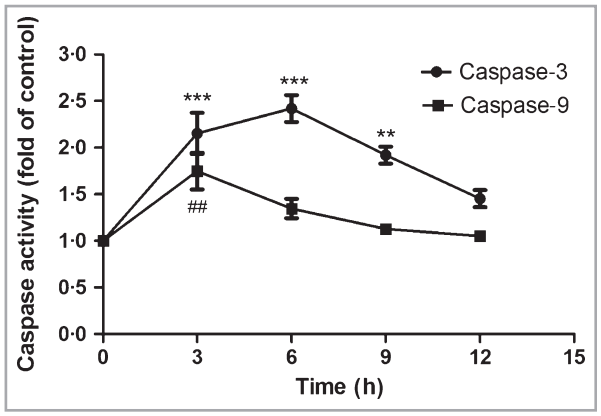

Fig 9. Activity of caspase-3 and caspase-9 in plasma-treated HaCaT cells. Cells with 3-min plasma treatment are collected for analysis at 3, 6, 9 and 12 h after treatment. The values are expressed as the fold change vs. control. $^{**}P < 0{\cdot}01$, $^{***}P < 0{\cdot}001$, $^{\#\#}P < 0{\cdot}01$.

cytokines on CAP dosage. It was found that CAP treatment induces significant release of IL-1β, IL-6, IL-8, IL-10, TNF-α, IFN-γ and VEGF at the protein or gene expression level. However, their CAP dose dependences are distinctly different. Most cytokines appear to follow an increasing trend with increasing treatment time, while the trend for IL-12 is by contrast a declining one. This appears to be the first evidence of CAP-induced cytokine release from keratinocytes, as well as its dose-dependent and cytokine-dependent character. One rare piece of evidence for plasma-induced cytokine release showed IL-6, IL-8, monocyte chemoattractant protein-1 and transforming growth factor-β1 release from dermal fibroblasts.[16] Increased production of IL-6 and IL-8 was observed for a single plasma treatment dose, but the dose–response relationship was not studied.[16]

Production of the proinflammatory cytokines IL-6, IL-8 and TNF-α is known to be high in patients with psoriasis,[35–37] whereas VEGF is thought to be a key factor in the link between inflammation and angiogenesis in psoriasis.[38] TNF-α, IFN-γ, IL-6, IL-8, IL-12 and IL-18 levels in serum of patients with psoriasis were found to be significantly higher than in controls, but a strong correlation with clinical severity and activity of psoriasis was established only with IFN-γ, IL-12 and IL-18.[39] IL-12 is therefore directly associated with clinical activity of psoriasis, with TNF-α, IL-6 and IL-8 having lesser clinical association. This is consistent with the fact that current systemic therapeutics for psoriasis vulgaris use IL-12 as a target.[40,41] In potential cytokine networks in psoriatic lesions, T-cell activation is thought to be through IL-12 or IL-23, leading to amplification of inflammation.[10] Taken together, these clinical and mechanistic studies highlight a central role of IL-12 and its supported candidacy as an effective therapeutic target. The statistically significant and progressive decline of IL-12 levels with increasing CAP doses offers preliminary yet encouraging evidence that CAP may possess therapeutic properties specific to treatment of psoriasis.

Regarding CAP-increased production of IL-6 and IL-8, it should be mentioned that their production *in vitro* is increased also with UVB irradiation,[42,43] and yet UVB is an effective therapeutic for psoriasis. The roles of IL-6, IL-8, TNF-α and VEGF therefore need to be studied much further both *in vitro* and *in vivo*. One aspect to be considered in future studies is their nonmonotonic dose–response curves, where different

Table 1 Mean ± SD concentrations of various cytokines in culture supernatants from dielectric-barrier discharge plasma-treated HaCaT cells (pg mL^{-1})

Group	IL-6	IL-8	IL-12	TNF-α	VEGF
Control	72·31 ± 11·94	596·92 ± 53·01	2·87 ± 0·33	0·92 ± 0·23	1587·96 ± 242·87
1 min	43·47 ± 2·37	378·11 ± 76·05	2·18 ± 0·21**	0·78 ± 0·20	2139·04 ± 287·29***
2 min	118·70 ± 20·41	1454·11 ± 245·42***	1·88 ± 0·12***	0·80 ± 0·15	2786·50 ± 428·14***
3 min	445·28 ± 36·94***	3996·40 ± 370·71***	2·02 ± 0·23**	2·54 ± 0·25***	2505·95 ± 349·49***

IL, interleukin; TNF, tumour necrosis factor; VEGF, vascular endothelial growth factor. $^{**}P < 0{\cdot}01$, $^{***}P < 0{\cdot}001$.

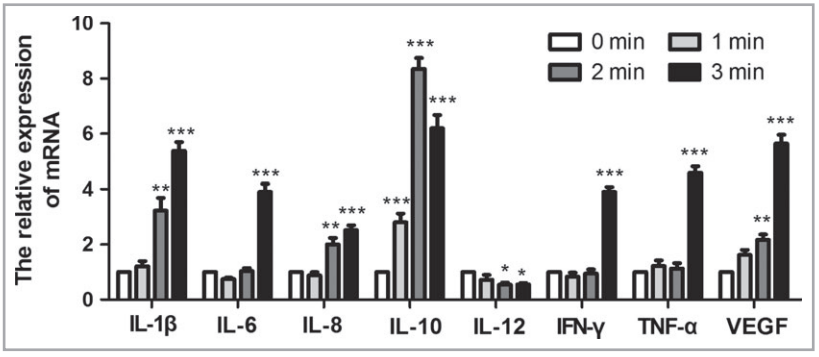

Fig 10. Effect of plasma treatment on mRNA levels of cytokines in HaCaT cells. $^{*}P < 0{\cdot}05$, $^{**}P < 0{\cdot}01$, $^{***}P < 0{\cdot}001$. IL, interleukin; IFN, interferon; TNF, tumour necrosis factor; VEGF, vascular endothelial growth factor.

time windows may be exploited for optimization using multiple plasma treatments.

In conclusion, DBD surface air plasma can induce cell death via apoptotic pathways with appropriate doses and can induce release of several psoriasis-relevant cytokines in a dose-dependent manner. Of particular interest is the progressive decrease of IL-12 with increasing plasma dose, as increased IL-12 production is known to be associated with both the clinical severity of psoriasis[31] and with T-cell activation, which directly contributes to amplification of inflammation.[10] Taken together, these points suggest that CAP with an appropriate composition and concentration of plasma agents may be used to enable effective suppression of keratinocyte hyperproliferation and the amplification of inflammation through inactivation of IL-12 and hence T-cell activation. These results are promising but need to be studied further with considerations of many aspects including interactions of cytokines in their network and the full immunology implication in an *in vivo* scenario. The option of manipulating the ROS/RNS dose and composition, as well as facilitating multiple rather than single time-windowed treatments, suggests a considerable scope to optimize the beneficial effects of physical plasmas for treatment of psoriasis.

Acknowledgments

We thank Mr Dong Li, Mr Qiaosong Li and Miss Miao Tian for technical support and helpful discussion.

References

1 Kong MG, Kroesen G, Morfill G *et al.* Plasma medicine: an introductory review. *New J Phys* 2009; **11**:115012.
2 Whittaker AG, Graham EM, Baxter RL *et al.* Plasma cleaning of dental instruments. *J Hosp Infect* 2004; **56**:37–41.
3 Isbary G, Morfill G, Schmidt HU *et al.* A first prospective randomized controlled trial to decrease bacterial load using cold atmospheric argon plasma on chronic wounds in patients. *Br J Dermatol* 2010; **163**:78–82.
4 Heinlin J, Isbary G, Stolz W *et al.* A randomized two-sided placebo-controlled study on the efficacy and safety of atmospheric non-thermal argon plasma for pruritus. *J Eur Acad Dermatol Venereol* 2013; **27**:324–31.
5 Isbary G, Heinlin J, Shimizu T *et al.* Successful and safe use of 2 min cold atmospheric argon plasma in chronic wounds: results of a randomized controlled trial. *Br J Dermatol* 2012; **167**:404–10.
6 Keidar M, Walk R, Shashurin A *et al.* Cold plasma selectivity and the possibility of a paradigm shift in cancer therapy. *Br J Cancer* 2011; **105**:1295–301.
7 Heinlin J, Isbary G, Stolz W *et al.* Plasma applications in medicine with a special focus on dermatology. *J Eur Acad Dermatol Venereol* 2011; **25**:1–11.
8 Fuchs J, Zollner TM, Kaufmann R, Podda M. Redox-modulated pathways in inflammatory skin diseases. *Free Radic Biol Med* 2001; **30**:337–53.
9 Reynolds NJ, Tranklin V, Gray JC *et al.* Narrow-band ultraviolet B and broad-band ultraviolet A phototherapy in adult atopic eczema: a randomized controlled trial. *Lancet* 2001; **357**:2012–16.
10 Lowes MA, Bowcock AM, Krueger JG. Pathogenesis and therapy of psoriasis. *Nature* 2007; **445**:866–73.
11 van Weelden H, De La Faille HB, Young E, van der Leun JC. A new development in UVB phototherapy of psoriasis. *Br J Dermatol* 1988; **119**:11–19.
12 Kusmartsev S, Nefedova Y, Yoder D, Gabrilovich DI. Antigen-specific inhibition of $CD8^+$ T cell response by immature myeloid cells in cancer is mediated by reactive oxygen species. *J Immunol* 2004; **172**:989–99.
13 Boukamp P, Petrussevska RT, Breitkreutz D *et al.* Normal keratinization in a spontaneously immortalized aneuploid human keratinocyte cell line. *J Cell Biol* 1988; **106**:761–71.
14 Fridman G, Shereshevsky A, Jost MM *et al.* Floating electrode dielectric barrier discharge plasma in air promoting apoptotic behavior in melanoma skin cancer cell lines. *Plasma Chem Plasma Process* 2007; **27**:163–76.
15 Lee HJ, Shon CH, Kim YS *et al.* Degradation of adhesion molecules of G361 melanoma cells by a non-thermal atmospheric pressure microplasma. *New J Phys* 2009; **11**:115026.
16 Arndt S, Wacker E, Li YF *et al.* Cold atmospheric plasma, a new strategy to induce senescence in melanoma cells. *Exp Dermatol* 2013; **22**:284–9.
17 Haertel B, Wende K, von Woedtke T *et al.* Non-thermal atmospheric-pressure plasma can influence cell adhesion molecules on HaCaT-keratinocytes. *Exp Dermatol* 2010; **20**:282–4.
18 Haertel B, Hahnel M, Blackert S *et al.* Surface molecules on HaCaT keratinocytes after interaction with non-thermal atmospheric pressure plasma. *Cell Biol Int* 2012; **36**:1217–22.
19 Haertel B, Straßenburg S, Oehmigen K *et al.* Differential influence of components resulting from atmospheric-pressure plasma on integrin expression of human HaCaT keratinocytes. *Biomed Res Int* 2013; **2013**:761451.
20 Blackert S, Haertel B, Wende K *et al.* Influence of non-thermal atmospheric pressure plasma on cellular structures and processes in human keratinocytes (HaCaT). *J Dermatol Sci* 2013; **70**:173–81.
21 Bundscherer L, Wende K, Ottmüller K *et al.* Impact of non-thermal plasma treatment on MAPK signaling pathways of human immune cell lines. *Immunobiology* 2013; **218**:1248–55.
22 Schmidt A, Wende K, Bekeschus S *et al.* Non-thermal plasma treatment is associated with changes in transcriptome of human epithelial skin cells. *Free Radic Res* 2013; **47**:577–92.
23 Wende K, Straßenburg S, Haertel B *et al.* Atmospheric pressure plasma jet treatment evokes transient oxidative stress in HaCaT keratinocytes and influences cell physiology. *Cell Biol Int* 2014; **38**:412–25.
24 Shi X-M, Zhang G-J, Yuan Y-K *et al.* Effects of low-temperature atmospheric air plasmas on the activity and function of human lymphocytes. *Plasma Process Polym* 2008; **5**:482–8.
25 Haertel B, Volkmann F, von Woedtke T, Lindequist U. Differential sensitivity of lymphocyte subpopulations to nonthermal atmospheric-pressure plasma. *Immunobiology* 2012; **217**:628–33.
26 Li D, Liu DX, Nie QY *et al.* Array of surface-confined glow discharges in atmospheric pressure helium: modes and dynamics. *Appl Phys Lett* 2014; **104**:204101–5.
27 Lunov O, Zablotskii V, Churpita O *et al.* Cell death induced by ozone and various non-thermal plasmas: therapeutic perspectives and limitations. *Sci Rep* 2014; **4**:7129.
28 Zhao M, Antunes F, Eaton JW, Brunk UT. Lysosomal enzymes promote mitochondrial oxidant production, cytochrome c release and apoptosis. *Eur J Biochem* 2003; **270**:3778–86.
29 Boya P. Lysosomal function and dysfunction: mechanism and disease. *Antioxid Redox Signal* 2012; **17**:766–74.
30 Temkin V, Karin M. From death receptor to reactive oxygen species and c-Jun N-terminal protein kinase: the receptor-interacting protein 1 odyssey. *Immunol Rev* 2007; **220**:8–21.

31 McKenzie RC, Sauder DN. The role of keratinocyte cytokines in inflammation and immunity. *J Invest Dermatol* 1991; **95**(6 Suppl.):105S–7S.
32 Ansel J, Perry P, Brown J *et al.* Cytokine modulation of keratinocyte cytokines. *J Invest Dermatol* 1990; **94**(6 Suppl.):101S–7S.
33 Barker JN, Mitra RS, Griffiths CE *et al.* Keratinocytes as initiators of inflammation. *Lancet* 1991; **337**:211–14.
34 Bulua AC, Simom A, Maddipati R *et al.* Mitochondrial reactive oxygen species promote production of proinflammatory cytokines and are elevated in TNFR1-associated periodic syndrome (TRAPS). *J Exp Med* 2011; **208**:519–33.
35 Neuner P, Urbanski A, Trautinger F *et al.* Increased IL-6 production by monocytes and keratinocytes in patients with psoriasis. *J Invest Dermatol* 1991; **97**:27–33.
36 Gillizer R, Berger R, Mielke V *et al.* Upper keratinocytes of psoriatic skin lesions express high levels of NAP-1/IL-8 mRNA *in situ*. *J Invest Dermatol* 1991; **97**:73–9.
37 Ettehadi P, Greaves MW, Wallach D *et al.* Elevated tumour necrosis factor-alpha (TNF-α) biological activity in psoriatic skin lesions. *Clin Exp Immunol* 1994; **96**:146–51.
38 Simonetti O, Lucarini G, Goteri G *et al.* VEGF is likely a key factor in the link between inflammation and angiogenesis in psoriasis: results of an immunohistochemical study. *Int J Immunopathol Pharmacol* 2006; **19**:751–60.
39 Arican O, Aral M, Sasmaz S, Ciragil P. Serum levels of TNF-α, IFN-γ, IL-6, IL-8, IL-12, IL-17, and IL-18 in patients with active psoriasis and correlation with disease severity. *Mediators Inflamm* 2005; **2005**:273–9.
40 Gottlieb AB, Griffiths CE, Ho VC *et al.* Oral pimecrolimus in the treatment of moderate to severe chronic plaque-type psoriasis: a double-blind, multicentre, randomized, dose-finding trial. *Br J Dermatol* 2005; **152**:1219–27.
41 Toichi E, Torres G, McCormick TS *et al.* An anti-IL12p40 antibody down-regulates type 1 cytokines, chemokines, and IL12/IL23 in psoriasis. *J Immunol* 2006; **177**:4917–26.
42 Chung JH, Youn SH, Koh WS *et al.* Ultraviolet B irradiation-enhanced interleukin (IL)-6 production and mRNA expression are mediated by IL-1α in cultured human keratinocytes. *J Invest Dermatol* 1996; **106**:715–20.
43 Kondo S, Kono T, Sauder DN, McKenzie RC. IL-8 gene expression and production in human keratinocytes and their modulation by UVB. *J Invest Dermatol* 1993; **101**:690–4.

Supporting Information

Additional Supporting Information may be found in the online version of this article at the publisher's website:

Fig S1. Trypan blue staining for 4-min plasma-treated HaCaT cells. All cells in the image were dead, as shown by positive staining for trypan blue.

Table S1. Sequences of the primers used for real-time polymerase chain reaction.